

Simulation Research on Ultrasonic Guided Waves Detection of Metal Rod Buffer System Bonding Quality

Yang Hu^{*1}, Wang Cheng²

¹National Key Laboratory for Electronic Measurement Technology,
North University of China, Taiyuan 030051, China;

²State Key Laboratory for Explosion Science and Technology,
Beijing Institute of Technology, Beijing 100081, China

*Corresponding author, e-mail: yanghu@nuc.edu.cn

Abstract

The judgment of metal rod buffer system bonding quality depends on the bond of the metal rods with the surrounding medium. System bonding area will lead to different reflection amplitude. Compared the simulation with the experiment, it can be concluded that different bonding area can measure bond quality, i.e., the greater the bonding area is the more excellent bonding quality will be. This conclusion provides the basis for the system ultrasonic testing.

Keywords: ultrasonic testing; bonding quality; simulation

Copyright © 2013 Universitas Ahmad Dahlan. All rights reserved.

1. Introduction

The judgment of metal rod buffer system bonding quality depends on the bond of the metal rods with the surrounding medium. In this paper, the concept of bonding area which will lead to different reflection amplitude is employed to measure the bonding quality. Response curve can be measured on site and it can show the amplitude of each reflected wave, which indicates the quantitative possibility to distinguish the metal rod bond quality. From the perspective of simulating finite element numerical, this paper performs thorough analysis and elaboration on the time domain response of the metal rod buffer system, and then obtains the relationship between the bonding area, bonding quality of the metal rod and its surrounding medium [1-3].

2. Model Establishment

2.1. Model Description

Figure 1 is the free metal pole model. Figure 2 is a metal rod buffer system model, which is divided into a steel layer, epoxy resin layer and the cement layer (simulated rock layer). The rod length is 1.5m, the diameter is 2cm, the bond length is 40cm. Basic parameter are shown in Table 1.

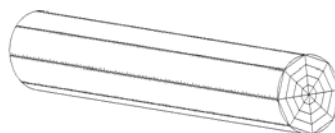


Figure 1. Free metal rod model

2.2. Model Flaw Descriptions

It is uncertain to identify flaw types of the scene metal rod cushion system, but as to its basic mode, it is poor bonding of metal pole with the surrounding rock or the falling off of the binder that causes the system to malfunction or fail.

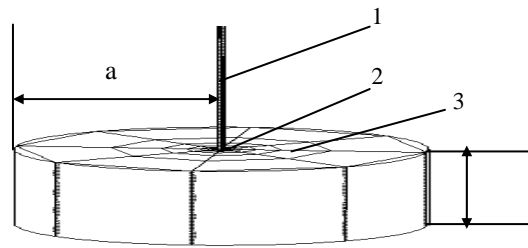
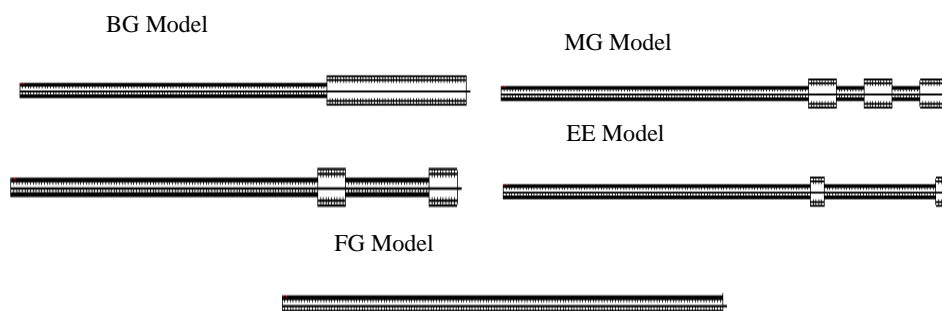


Figure 2. Metal rod buffer system model
1 metal rod 2 resin level 3 layers of cement

Table1. Basic parameters of metal rods buffer system's numerical model

	Elastic modulusE(Gpa)	Poisson ratio μ	Density ρ (kg/m ³)	Diameter Φ (cm)	Length L(cm)
Metal rod	206	0.25	7900	2	150
Resin level	14	0.30	2000	4(Outer diameter)	40
Layers of cement	40	0.29	2520	4(Outer diameter)	40

In this paper, the flaw degree can be obtained by calculating the area of bonding of metal rod with its surrounding rock, the metal rod buffer system of different bonding quality can be simulated by establishing four kinds of finite element models with different bonding area buffer system [4- 7]. Bonding quality is categorized into: excellent, good, fair, poor, represented respectively by BG, MG, CC and EE. And metal rod models are also created, represented by FG. As shown in Figure 3, after removing the cement outer layer, four finite element molded graphs of the resin level and the metal rod with different bonding quality are left behind, namely BG model (to simulate the best bonding quality, 100% of the area is completely bonded), MG model (to simulate the better bonding quality, 70% of the area is completely bonded), CC model (to simulate the good bonding quality, 40% of the area is completely bonded), EE model (to simulate poor bonding quality, 20% of the area is completely bonded), and FG model (to simulate the free metal rod, 20% of the area is completely bonded).



3. Simulation Analysis

Figure 4 is the system acceleration time-domain response curve. Excited guided wave goes along the metal rod and spreads outward at the central hemispherical radial direction. It is quite complex to spread at the top. When the wave goes along the rod to a certain distance s (according to the Saint-Venant principle, $S > 1 \sim 2D$, D is the metal rod diameter), the

wavefront then is approximate to plane dissemination. Therefore, when gathering signals from the rod's central point, the front signal should be zero.

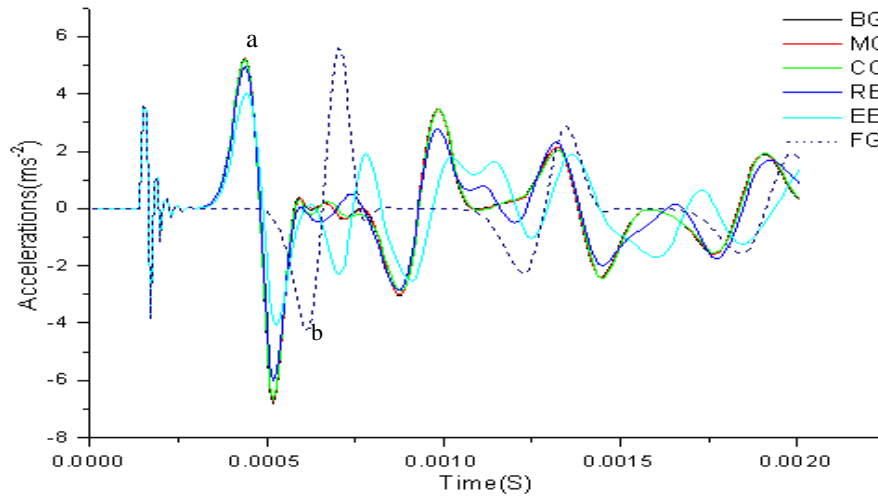


Figure 4. Acceleration time-domain response graph

Table 2. Data point a in Figure 4

Data (point a)	BG Model	MG Model	CC Model	EE Model
Time(μ s)	438	439	438	439
Amplitude (ms^{-2})	5.26941	5.24098	5.22515	4.94928

In Figure 4, point a is the reflection point on the interface of the solid side. We can calculate the speed of wave transmission in the rod as follows:

$$c_a = \frac{1.1 \times 2}{4.37e-4} = 5034.32ms^{-1}$$

Point b is the free metal rod at the bottom of the reflected wave, $b=623s$, the speed of wave transmission in the rod is

$$c_b = \frac{1.6 \times 2}{6.23e-4} = 5136.43ms^{-1}$$

And, according to the material properties, the calculated theoretical rod speed is $c_0 = \sqrt{\frac{E}{\rho}} = \sqrt{\frac{2.06e11}{7900}} = 5106.46ms^{-1}$. Relative error is $\frac{|5106.46 - 5034.32|}{5106.46} = 1.46\%$,

$\frac{|5106.46 - 5136.43|}{5106.46} = 0.58\%$, which are very small. In order to observe the wave

transmission in different models, we enlarge the reflection point area of the third solid side on the interface, as shown in Figure 5. It can see that with model bonding quality decreasing, the waveform is in turn close to the free rod waveform and its phase back offset. This obvious change of varying with different bonding quality reveals the reliability of finite element model.

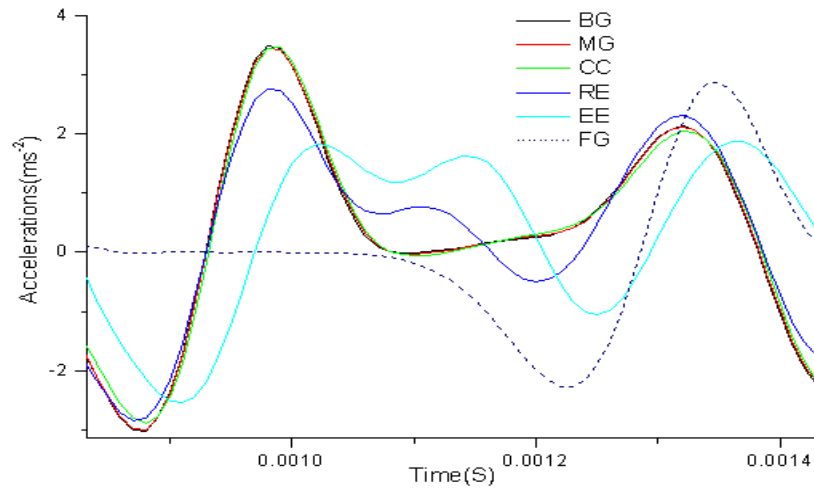


Figure 5. Each model reflection region enlargement of the interface on the third solid side

3.1. Relationship Between Bonding Area and Amplitude Attenuation

Model bonding length is set to 40 CM (FG Model Glue size is 0). The different bonding area leads to different amplitude attenuation. There must exist a relationship between the bonded area and amplitude attenuation. We collect the curve data that at equidistant the center point of the interface on the solid side and bottom center points of each model, put them together, and then we get a response chart of corresponding time domain, as shown in Figure 6 and 7.

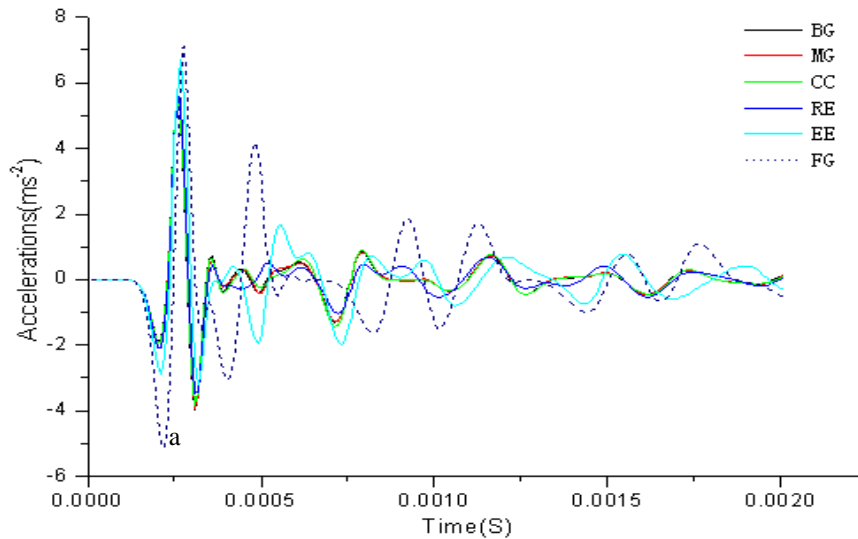


Figure 6. Time-domain map of the equidistant center point on the model fixed end interface

In Figure 6 waveform oscillation amplitude is relatively large, while in Figure 7, the waveform oscillation amplitude is significantly small, which reflects the attenuation of the energy to reach the bottom of the process. a, b are the first wave spots of each model. We can calculate the attenuation of bonding segment of each model, as shown in Figure 8 and Table 3.

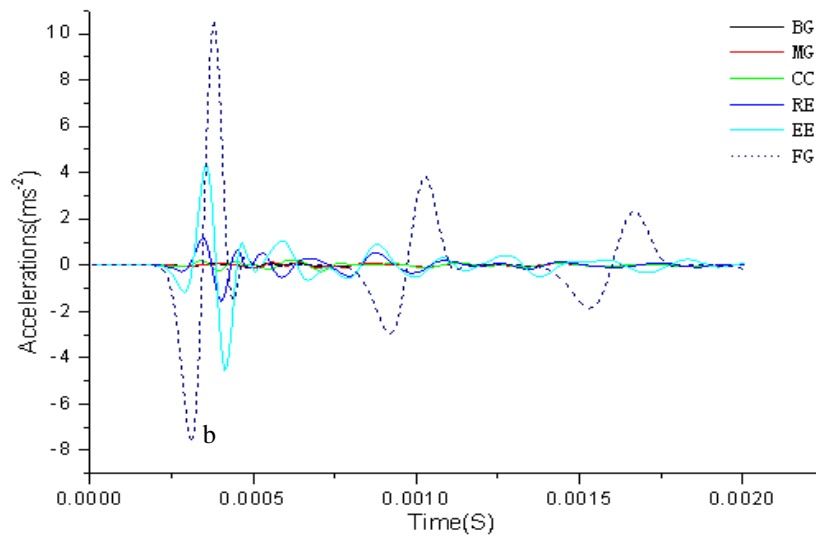


Figure 7. Time-domain chart of the model bottom center point

Table 3. Each model bonding segment amplitude attenuation

Data	BG Model	MG Model	CC Model	EE Model	FG Model
Amplitude attenuation (%)	99.2%	98.97%	98.37%	93.28%	25.17%
Bonding area (%)	100%	70%	40%	20%	0

From the fitting curve in Figure 8, it can see that the bonding segment amplitude attenuation is nonlinear, similar to the attenuated form of the exponential function. When bonding area is between 0% -40%, amplitude attenuation changes significantly, but when the bonding area between is 40% -100%, its change is insignificant, which explains why the BG and MG model curve in Figure 4 are close to good distinguishing; whereas CC, RE, and FG model of the three curves so significantly differ. It can be concluded that the acceleration domain curve in Figure 4 can basically separate these two sets of bonding quality of the bonding area 100% - 40% and 40% -0%, therefore, verifying that it is feasible to tell the pros and cons of the bonding quality by bonding area and furthermore can reflect the quality status of the metal rod bonding on site.

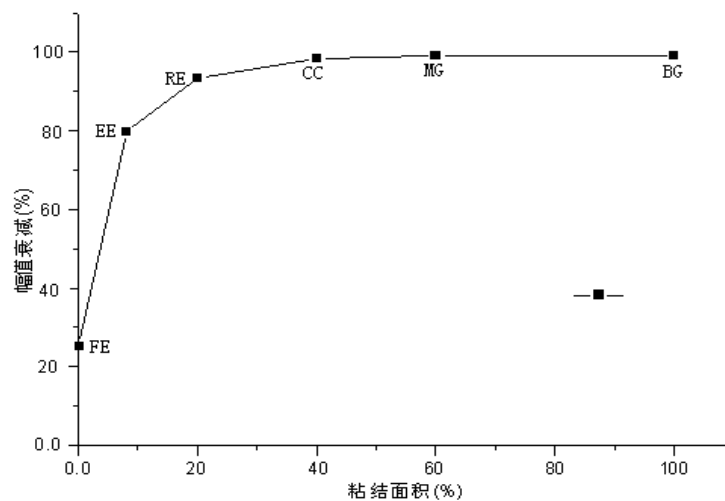


Figure 8. Amplitude attenuation and the bonding area relation graph

4. Comparison of Simulation and Test Data

4.1. Test Description

The free metal rod experiment uses the field used buffer rod at length $L=1.5\text{m}$ and diameter $\varphi=2\text{cm}$. When in experiment, it is at the free state. Metal rod buffer system test takes the representative medium's stable rock layer as the simulation object. The rock mass is designed as $0.6\times 0.5\times 0.5\text{m}^3$ concrete cube, with bonding length 40cm , metal rod length $L=1.5\text{m}$, and the intermediate deck uses epoxy resin.

4.2. Results Analysis

As shown in Figure 9, the supposed metal rod bottom end reflection time is T_0 ; the metal rod length is L_0 , the bonding length is L ; the fixed end interface reflection is T . If the average velocity of guided wave in metal rod is v_0 , then $T_0 = 2L_0/v_0$, $T = 2(L_0 - L)/v_0$.

Through the experiment $v_0 = 5161\text{ms}^{-1}$. Simulation and experimental data obtained are shown in Table 4. It can see that the numerical simulation values of the critical reflection point and the experimental value are basically in agreement.

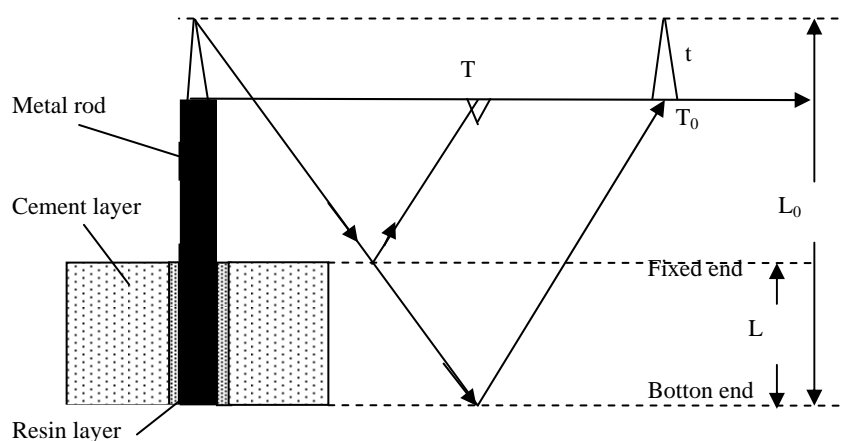


Figure 9. Metal rod system fluctuation diagram

Table 4. Time value of the solid side interface reflection point and the bottom reflection point

Time value of numerical simulation $T(\mu\text{s})$	Time value of experimental test $T(\mu\text{s})$
622	621
623	620
466	468

5. Conclusion

Comparative analysis of the simulation results and experimental data comes to the following conclusions:

- 1) The size of the bonding area can be a true reflection of the size of the bond quality on site. The difference of the energy amplitude attenuation resulting from the difference of the bonding quality provides a scientific calibration method for simulation study.
- 2) Finite element simulation and theoretical results can clearly identify the interface reflection on the fixed end point but fail to identify the bottom reflection point. Simulation and experimental results coincide well. The subtle difference is that the experimental curve

appears to jitter, which is caused by the interference of the field test instrument. Hence, the simulation results are reliable .

- 3) Energy attenuation is the reason why the bottom reflection wave can not be clearly identified, but it can clearly identify the reflected wave on the interface of the solid side. We can determine the bonding quality of the system through the amplitude of the reflected wave.
- 4) It can be ideal to simulate by using the finite element software. This will provide a strong technical support for more in-depth study.

References

- [1] MD Beard, MJS Lowe. Non-destructive testing of rock bolts using guided ultrasonic waves. *International Journal of Rock Mechanics, Mining Sciences*. 2003; 40: 527-536.
- [2] Beard MD, Lowe MJS, Cawley P. Ultrasonic guided waves for the inspection of grouted tendons and bolts. *J Mater Civil Eng*. 2002, in press.
- [3] BN Pavlakovic, MJS Lowe, P Cawley. High-frequency low-loss ultrasonic modes in imbedded bars. *Journal of Applied Mechanics*. 2001; 68: P67-65.
- [4] Paulus Insap Santosa. Cost and Benefit of Information Search using Two Different Strategies. *TELKOMNIKA Indonesian Journal of Electrical Engineering*. 2010; 8(3): 196-199.
- [5] Roy BVB Simorangkir, Achmad Munir. Numerical Design of Ultra-Wideband Printed Antenna for Surface Penetrating Radar Application. *TELKOMNIKA*. 2011; 9(2): 341-350.
- [6] Wu Bin, Sun Yaxin, He Cunfu, Wang Xiuyan ect. Application of high frequency ultrasonic guided waves to inspection of full-length-bonding bolt. *Chinese Journal of Rock Mechanics and Engineering*. 2006; 25(6): 1 240-1 245.
- [7] FQ Guo and CS Zhang. Review of research on non-destructive testing of bonding quality of grouted rock bolt (in Chinese). *Journal of Taiyuan university of Technology*. 2005; 36: 11-14 (Sup.).
- [8] Chung-Hsin Liu, Po-Ching Teng. The Study for Home Surveillance Fuzzy Control System of Attacks Analysis. *JCIT: Journal of Convergence Information Technology*. 2011; 6(11): 30- 40.
- [9] J Alamelu Mangai and S Sameen Fathima Appavu alias Balamurugan. Feature Selection for Large Scale Data Using Class Association Rule Mining. *JCIT: Journal of Convergence Information Technology*. 2011; 6(11): 371- 377.
- [10] Written by JL Rose. Translated by He Cun-fu, Wu Bin, Wang Xiu-Yan, Checked by Yang Gui-tong. *Ultrasonic Waves in Solid Media*. Beijing: Science Press. 2004; 3: 14-16.
- [11] JL Ross. *Solids Ultrasonic*. Science Press, Beijing China. 2004: 14-17.